

Improvement of $N_f = 3$ lattice QCD with Wilson fermions and tree-level improved gauge action

John Bulava^{a,b} and Stefan Schaefer^a

^a CERN, Physics Department, 1211 Geneva 23, Switzerland

^b School of Mathematics, Trinity College, Dublin 2, Ireland

Abstract

We determine the parameter c_{SW} required for $O(a)$ -improvement of the three flavor Wilson fermion action together with the tree-level Symanzik improved gauge action. The standard improvement condition is employed for a range of couplings. Additionally, we perform a check of the volume independence of c_{SW} and provide a preliminary estimate of the lattice spacing at our largest values of g_0^2 .

Key words: Lattice QCD; Non-perturbative improvement

PACS: 12.38.Gc

1 Introduction

The continuum limit is an essential part of lattice QCD calculations. In order to control this extrapolation in the lattice spacing a , it is advisable to work with a discretization whose leading cut-off effects are $O(a^2)$. The theory and reduction of scaling violations in on-shell quantities is well-established [1,2,3] and for Wilson fermions [4] $O(a)$ improvement can be achieved by adding a single dimension-five operator to the action [5]. This requires the non-perturbative tuning of its coefficient c_{sw} and can be performed using a standard procedure [6,7]. Simulations with the resulting action in two-flavor flavor QCD have exhibited the expected moderate scaling violations [8].

Here we present a determination of the coefficient c_{sw} using the standard procedure for $N_f = 3$ flavor QCD with the tree-level improved Lüscher–Weisz gauge action [9]. We choose this gauge action because it has been demonstrated to possess superior scaling properties in pure gauge theory [10].

This paper is organized as follows. After defining our lattice regularization in Sec. 2, we summarize the standard improvement programme in Sec. 3. In Sec. 4 details of the numerical computations are given together with the resultant interpolating formula for the improvement coefficient $c_{\text{sw}}(g_0^2)$. We also give results for a renormalized quantity which suggests that the range of bare couplings covered by our simulations extends at least to a lattice spacing of $a \approx 0.09$ fm.

2 Lattice setup

The $O(a)$ -improved Wilson Dirac operator [4,5] is given by

$$D_W = \frac{1}{2} \sum_{\mu=0}^3 \{ \gamma_\mu (\nabla_\mu^* + \nabla_\mu) - \nabla_\mu^* \nabla_\mu \} + c_{\text{sw}} \sum_{\mu,\nu=0}^3 \frac{i}{4} \sigma_{\mu\nu} \widehat{F}_{\mu\nu} + m_0 \quad (2.1)$$

with ∇_μ and ∇_μ^* the covariant forward and backward derivatives, respectively, and $\widehat{F}_{\mu\nu}$ the standard discretization of the field strength tensor [11]. The bare mass m_0 will be replaced below by the hopping parameter κ with $m_0 = (\kappa^{-1} - 8)/2$.

The gauge action S_G contains sums over all oriented 1×1 plaquettes as well as all 1×2 rectangles, which are denoted by the sets \mathcal{S}_0 and \mathcal{S}_1 , respectively,

$$S_G = \beta \sum_{k=0,1} c_k \sum_{\mathcal{C} \in \mathcal{S}_k} w_k(\mathcal{C}) \text{tr}\{1 - U(\mathcal{C})\}, \quad (2.2)$$

where $\beta = 6/g_0^2$, $c_0 = 5/3$ and $c_1 = -1/12$. The weight factor $w_k(\mathcal{C})$ is set to unity for all loops away from the boundaries. Schrödinger functional [12,13] boundary

conditions are imposed on the gauge fields such that

$$w_0(\mathcal{C}) = \begin{cases} \frac{1}{2}, & \text{all links in } \mathcal{C} \text{ are on a boundary} \\ 1, & \text{otherwise} \end{cases} \quad (2.3)$$

and

$$w_1(\mathcal{C}) = \begin{cases} \frac{1}{2}, & \text{all links in } \mathcal{C} \text{ are on a boundary} \\ \frac{3}{2}, & \mathcal{C} \text{ has exactly two links on a boundary} \\ 1, & \text{otherwise.} \end{cases} \quad (2.4)$$

This corresponds to ‘Choice B’ of Ref. [14] and guarantees boundary $O(a)$ improvement at tree-level of perturbation theory. We also set the fermionic boundary counter term according to the 1-loop formula [14]

$$c_F = 1 - 0.0122 C_F g_0^2, \quad \text{with } C_F = 4/3. \quad (2.5)$$

Finally, the values of the spatial links at the boundaries are fixed to

$$U(x, k)|_{x_0=0} = \exp\{aC_k\}, \quad C_k = \frac{i}{6L} \text{diag}(-\pi, 0, \pi), \quad (2.6)$$

$$U(x, k)|_{x_0=T} = \exp\{aC'_k\}, \quad C'_k = \frac{i}{6L} \text{diag}(-5\pi, 2\pi, 3\pi), \quad (2.7)$$

while the fermion fields satisfy periodic boundary conditions in the spatial directions and the standard Schrödinger functional boundary conditions in time.

3 Improvement condition

The standard $O(a)$ improvement programme relies on the PCAC relation, which involves the improved axial-vector current $(A_I)_\mu^a$ and the pseudoscalar density P^a given by

$$(A_I)_\mu^a = A_\mu^a + a c_A \frac{1}{2} (\partial_\mu^* + \partial_\mu) P^a, \quad (3.1)$$

$$A_\mu^a(x) = \bar{\psi}(x) \gamma_\mu \gamma_5 \frac{\lambda^a}{2} \psi(x), \quad P^a(x) = \bar{\psi}(x) \gamma_5 \frac{\lambda^a}{2} \psi(x). \quad (3.2)$$

In the unimproved theory the unrenormalized PCAC relation

$$\frac{1}{2} (\partial_\mu + \partial_\mu^*) \langle (A_I)_\mu^a(x) \mathcal{O} \rangle = 2m \langle P^a(x) \mathcal{O} \rangle \quad (3.3)$$

is violated by terms of $O(a)$. By using three different choices of x , \mathcal{O} and \mathcal{O}' one can define c_{sw} and c_A , requiring that m is the same in all three cases. In this situation Eq. 3.1 holds up to $O(a^2)$.

This method has been applied to the $N_f = 0, 2, 3, 4$ cases for a variety of different actions [6,7,15,16,17,18]. For technical reasons, we use lattices with $T = 2L - a$. However, this additional $O(a)$ effect is irrelevant, as the determination of c_{sw} using our improvement condition is ambiguous at $O(a)$. We employ the PCAC relation with boundary operators \mathcal{O} and \mathcal{O}' on time slices $x_0 = 0$ and $x_0 = T$, respectively,

$$\mathcal{O}^a = a^6 \sum_{\mathbf{y}, \mathbf{z}} \bar{\zeta}(\mathbf{y}) \gamma_5 \frac{\lambda^a}{2} \zeta(\mathbf{z}), \quad \mathcal{O}'^a = a^6 \sum_{\mathbf{y}, \mathbf{z}} \bar{\zeta}'(\mathbf{y}) \gamma_5 \frac{\lambda^a}{2} \zeta'(\mathbf{z}). \quad (3.4)$$

The correlation functions which enter the PCAC relation Eq. 3.1 are then

$$f_A(x_0) = -\frac{1}{3} \langle A_0^a(x) \mathcal{O}^a \rangle, \quad f_P(x_0) = -\frac{1}{3} \langle P^a(x) \mathcal{O}^a \rangle, \quad (3.5)$$

$$f'_A(T - x_0) = +\frac{1}{3} \langle A_0^a(x) \mathcal{O}'^a \rangle, \quad f'_P(T - x_0) = -\frac{1}{3} \langle P^a(x) \mathcal{O}'^a \rangle, \quad (3.6)$$

As has been suggested in Ref. [6], effective masses $M(x_0)$ defined by

$$M(x_0, y_0) = r(x_0) - s(x_0) \frac{r'(y_0) - r(y_0)}{s'(y_0) - s(y_0)}. \quad (3.7)$$

with

$$r(x_0) = \frac{1}{4} (\partial_0^* + \partial_0) f_A(x_0) / f_P(x_0) \quad \text{and} \quad s(x_0) = \frac{1}{2} a \partial_0^* \partial_0 f_P(x_0) / f_P(x_0) \quad (3.8)$$

correspond to a particular choice of c_A in the improved currents. Since $M(x_0, y_0)$ renormalizes multiplicatively, it is a useful quantity to define the quark mass at fixed β and c_{sw} . Specifically, we take as our definition of the quark mass

$$M = \frac{1}{2} (M(L, L/2) + M(L - a, L/2)). \quad (3.9)$$

Tuning $M \approx 0$ defines the values of κ at which we impose the improvement condition.

As discussed above, this improvement condition requires the difference between two masses to vanish. In addition to $M(x_0, y_0)$, a second mass $M'(x_0, y_0)$ is considered where r and s in Eq. 3.7 are replaced by their primed counterparts. These masses are evaluated at $x_0 = 3T/4$ and $y_0 = T/4$. However, because we have $T = 2L - a$, we round the two arguments towards the center of the lattice.

The parameter c_{sw} is chosen such that the difference between these two masses ΔM is equal to its tree-level value $\Delta M^{(0)}$

$$\Delta M = M(3T/4, T/4) - M'(3T/4, T/4) \equiv \Delta M^{(0)}. \quad (3.10)$$

The numerical value of $\Delta M^{(0)}$ depends on the lattice geometry and can be computed using the solution to the Dirac equation as given in Sec. 6.2 of Ref. [19]. For the 15×8^3 lattices $a\Delta M^{(0)} = 0.000393$. Additionally, this offset may be obtained from measurements on free gauge fields. A stringent test of our entire workflow is the reproduction of the $\Delta M^{(0)}$ obtained from analytic calculations using simulations at large values of β .

In principle it would be preferable to keep the physical size of the system L constant as the continuum limit is approached. This, however, turns out to be very costly in practice, because autocorrelations associated with the topological charge sectors quickly become very large as the lattice spacing is lowered. We therefore opt to impose the improvement condition at fixed L/a , where the contribution of non-zero topological charge sectors decreases rapidly in the continuum limit. In Sec. 5.3 we will show that the effect of the finite volume does not seem to be relevant at the current level of accuracy.

4 Simulations

For the simulations we use the `openQCD` code, which is publicly available online¹ and implements the lattice setup of Sec. 2 for several simulation algorithms. These algorithms are the subject of Ref. [20] so we restrict ourselves to a brief summary here.

We employ the HMC algorithm [21] with a twisted-mass Hasenbusch frequency splitting [22,23] for a doublet of two of the three degenerate quarks. For most ensembles with $\beta \leq 3.5$ twisted mass reweighting [24] is used, i.e. we simulate with a small twisted mass $\mu = 0.001$ and then include a stochastically estimated reweighting factor to correct for this in the measurement. This significantly increases the stability of the simulation. The third quark is simulated using the RHMC algorithm [25]. In all cases, we use a nine pole rational approximation in the interval $[0.02, 7.2]$ and correct for the rational approximation with an additional stochastically estimated reweighting factor. All fermion determinants are factorized using even-odd preconditioning.

For the entire range of couplings, we generated 15×8^3 lattices at a variety of c_{sw} values listed in Table 1. In addition, 23×12^3 ensembles at $\beta = 3.8$ have been

¹<http://luscher.web.cern.ch/luscher/openQCD>

generated as finite volume checks. To obtain a preliminary estimate of the lattice spacing at $\beta = 3.3$ and 3.4 , we performed some $L = T$ runs (using a modified version of the `openQCD` code) with $L/a = 8$ and zero boundary fields. These runs used both our discretization and the one of Ref. [26] and are summarized in Table 3.

For the $L/a = 8$ lattices at the four smallest values of β we use a three-level hierarchical integration scheme in which the outermost level employs the second order Omelyan-Mryglod-Folk (OMF) integrator, while the two inner levels use the fourth order OMF integrator [27]. The force from the pole closest to the origin in the rational approximation is integrated on the coarsest timescale, the remaining fermion forces on the intermediate timescale, and the gauge force on the finest timescale. Four or five outermost iterations together with a single iteration of the remaining two integrators typically achieve $\approx 90\%$ acceptance for molecular dynamics trajectories of length $\tau = 2$.

For the $L/a = 12$ runs at $\beta = 3.8$, the remaining $L/a = 8$ runs and the $T = L$ runs, a two level scheme with both levels using fourth order OMF was found to be effective, with between 5 and 8 steps in the outermost integrator and a single inner iteration.

The integration schemes discussed above were very stable in all cases, resulting in small Hamiltonian violations. The most difficult simulations were those with $L/a = 8, T = 2L - a$ at $\beta = 3.3$ at the smallest value of c_{sw} , but even those had only about 0.6% trajectories with $\Delta H > 10$. At $c_{\text{sw}} = 2.1$ this falls already to 0.2% and we had 0.08% of such events at $c_{\text{sw}} = 2.4$. At the smallest $c_{\text{sw}} = 1.7$ for $\beta = 3.4$ these trajectories occurred with 0.1%, a percentage rapidly falling for larger values of c_{sw} and β .

5 Results

We finally come to the results of our simulations. Our analysis strategy is discussed in Sec. 5.1 and results for $c_{\text{sw}}(g_0^2)$ are collected in Sec. 5.2, with a finite volume check in Sec. 5.3. A preliminary scale determination is given in Sec. 5.4.

A summary of the ensembles generated for the determination of c_{sw} appears in Tab. 1, where we also give the total statistics accumulated over several replica. These ensembles consist of $L/a = 8$ lattices used for our final result as well as those used for the finite volume check. The ensembles generated for the preliminary scale setting are discussed in Sec. 5.4 and collected in Tab. 3.

β	L/a	c_{sw}	κ	aM	$a\Delta M$	MDU
3.3	8	1.80	0.1434558	-0.0092(16)	0.0028(8)	75622
		2.10	0.1372440	-0.0010(12)	-0.0006(10)	54336
		2.40	0.1315404	0.0036(6)	-0.0013(4)	39002
		2.70	0.1266163	0.0101(4)	-0.0042(3)	33104
3.4	8	1.70	0.1427535	-0.0018(9)	0.0015(11)	135310
		2.00	0.1371025	-0.0125(6)	-0.0001(4)	115036
		2.30	0.1318818	-0.0089(5)	-0.0021(3)	53282
		2.60	0.1270442	0.0070(3)	-0.0050(2)	63136
3.5	8	1.85	0.1374470	0.0091(7)	0.0004(4)	48860
		2.20	0.1319060	0.0010(3)	-0.0020(2)	62872
		2.55	0.1267940	0.0109(4)	-0.0056(3)	37800
3.601	8	1.50	0.1420500	-0.0009(14)	0.0030(7)	19200
		1.70	0.1387200	-0.0057(9)	0.0006(5)	22200
		1.90	0.1353560	-0.0010(6)	-0.0002(4)	20200
		2.10	0.1319920	0.0130(4)	-0.0027(3)	28600
3.8	8	1.20	0.1434300	0.0134(10)	0.0039(5)	47400
		1.40	0.1405500	0.0041(7)	0.0023(5)	21942
		1.60	0.1376520	0.0006(5)	0.0011(3)	25762
		2.00	0.1319400	0.0043(4)	-0.0029(2)	43986
3.8	12	1.20	0.1434300	0.0095(5)	0.0012(3)	14967
		1.60	0.1376520	0.0005(3)	0.0003(2)	7000
		2.00	0.1319220	0.00952(15)	-0.00095(16)	12500
4.3	8	1.00	0.1410350	0.0071(13)	0.0045(5)	6166
		1.30	0.1374570	0.0053(5)	0.0015(4)	6598
		1.60	0.1342250	-0.0035(5)	-0.0010(4)	5200
		1.90	0.1311370	-0.0144(7)	-0.0042(4)	6400
6.0	8	1.00	0.1341200	-0.00058(20)	0.0029(3)	6400
		1.20	0.1324830	0.00517(16)	0.00053(14)	7180
		1.40	0.1310350	0.00394(17)	-0.00174(13)	6938
		1.60	0.1296320	0.00118(11)	-0.00397(11)	7174

Table 1: Simulation parameters for the runs used in the c_{sw} determination as well as the resultant values for aM and $a\Delta M$ calculated on those ensembles. The integrated molecular dynamics time of all replica for each ensemble is also given. For all of these runs the boundary fields are as specified in Eq. 2.6.

β	3.3	3.4	3.5	3.601	3.8	4.3	6.0
c_{SW}	2.13(5)	1.96(4)	1.90(3)	1.78(3)	1.61(2)	1.43(2)	1.213(9)

Table 2: Values of the optimal c_{SW} for which $a\Delta M = a\Delta M^{(0)}$. Each value is from a linear interpolation of $L/a = 8$ data at a fixed value of β .

5.1 Analysis

For each value of the coupling, we have to find the value of c_{SW} and the quark mass for which the improvement condition is satisfied. It has already been shown in the past that the condition $M = 0$ does not have to be achieved to a very high accuracy [7,17] and we therefore require $|aM| < 0.015$ for each individual point. We then measure $a\Delta M$ for several choices of c_{SW} and interpolate linearly to find the point with $\Delta M = \Delta M^{(0)}$.

The measurements of the required fermionic correlation functions (Eq. 3.5) are separated by one trajectory of length $\tau = 2$. Using the methods and software of Ref. [28], we determine the integrated autocorrelation times of the observables aM and $a\Delta M$ and find them to be at most around 8 units of molecular dynamics time such that all ensembles provide at least 500 independent measurements and thus a reliable determination of the errors. This is confirmed by the normal distribution of mean values on single replica.

Also, by studying the observables defined through the Wilson flow [29] — the action density constructed from smoothed links and the topological charge — we ensure that field space is sufficiently sampled in all simulations. In particular the topological charge is known to cause problems in the continuum limit [30]. However, since we keep L/a fixed instead of L , the contribution of sectors of non-zero topological charge diminishes rapidly as $a \rightarrow 0$.

The integrated autocorrelation times of the smoothed action and the topological charge at various smoothing ranges do not exceed 100 units of molecular dynamic time in any of our simulations. We therefore conclude that also for these observables configuration space is sampled sufficiently.

5.2 c_{SW} for $L/a = 8$

The results for the improvement condition as a function of c_{SW} as well as the resultant linear interpolations are shown in Fig. 1 for six values of β . The level of statistics is such that c_{SW} is determined with better than 3% precision in all cases. The optimal c_{SW} values at fixed β are collected in Tab. 2 and shown in

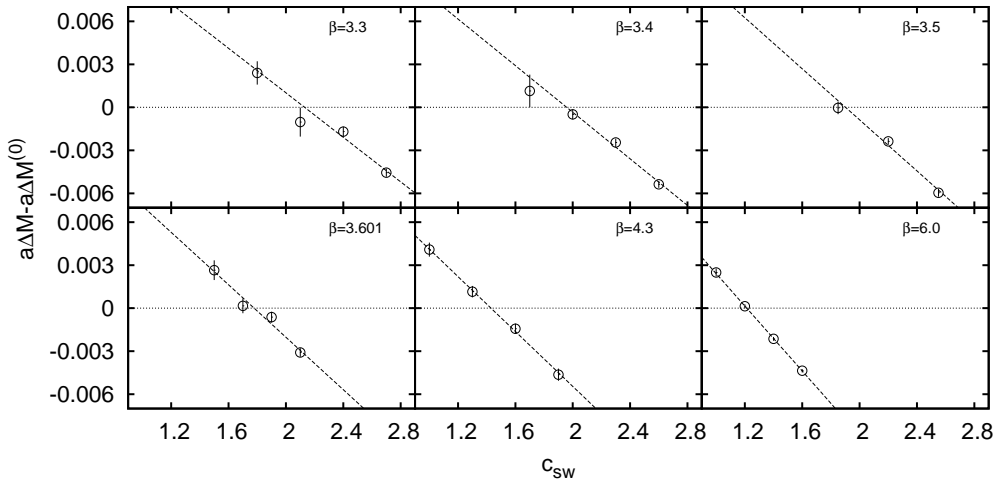


Figure 1: The improvement condition ΔM for several values of c_{SW} at each value of β . Linear fits to the improvement condition as a function of c_{SW} at fixed β are also shown. The resultant values of c_{SW} which minimize the improvement condition are given in Table 2.

Fig. 2 together with the best-fit interpolating curve

$$c_{\text{SW}}(g_0^2) = \frac{1 - 0.1921 g_0^2 - 0.1378 g_0^4 + 0.0717 g_0^6}{1 - 0.3881 g_0^2}. \quad (5.1)$$

We see that the fit describes the data well and that the data approaches the known 1-loop result at large β , which we use to constrain the interpolating curve.

5.3 Finite volume check

Although c_{SW} has typically been determined at fixed $L/a = 8$, it is interesting to assess the impact of this choice on the final result. As stated above, it would actually be preferable to keep L fixed when imposing the improvement condition. Smaller volumes are advantageous as they are computationally cheaper and have a larger slope in ΔM vs. c_{SW} , resulting in a clearer signal. Also, the problem of autocorrelations associated with freezing topological modes is much reduced. However, small volumes give rise to potentially large $O(a)$ effects in c_{SW} .

We detail here a single check at $\beta = 3.8$ between $L/a = 8$ and $L/a = 12$. The result is shown in Fig. 3. Within the statistical accuracies, the two volumes give the same value of c_{SW} . With $c_{\text{SW}} = 1.64(2)$ for $L/a = 8$ and $1.61(5)$ for $L/a = 12$,

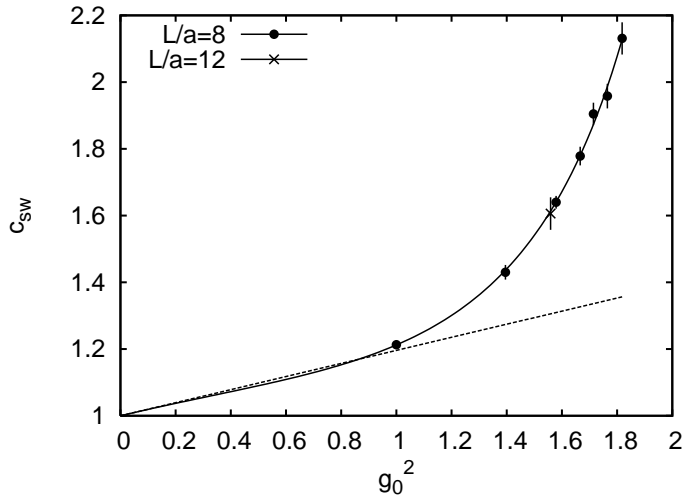


Figure 2: Calculated values for c_{sw} together with the interpolating function represented by the solid line. The dashed line is given by one-loop perturbation theory. To quantify finite volume effects, a value from simulations at 23×12^3 is given, with the value for g_0^2 slightly shifted to the left for clarity.

one can conclude that at least up to that lattice spacing, the smaller lattices are a good choice for the determination of c_{sw} . The point at $L/a = 12$ also does not deviate by more than one standard deviation from the interpolating curve plotted in Fig. 2. Therefore, given our statistical accuracy, the systematic effects from fixing $L/a = 8$ do not appear to be significant.

5.4 Preliminary scale determination

To estimate the lattice spacing we compute a quantity with our discretization as well as the discretization used by PACS-CS, where the scale is known from large volume simulations using the mass of the Ω baryon [31]. For comparison we use the coupling defined in Ref. [32], except with periodic spatial boundary conditions for the fermion fields, i.e. with $\theta = 0$. This coupling is a renormalized quantity and at $M = 0$ depends only on L , up to scaling violations. This lattice size L at a given value of the coupling serves as the dimensionful quantity to set the physical scale.

Our results for this coupling are tabulated in Table 3. In both discretizations we expect cutoff effects of order $O(ag_0^2)$ as boundary improvement for the gauge fields is implemented at tree level only. Furthermore, boundary improvement for

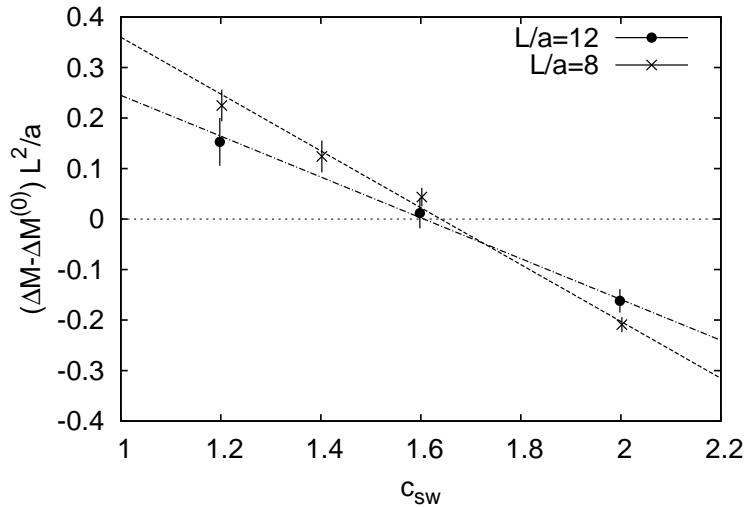


Figure 3: A comparison of the improvement condition at $L/a = 8$ and $L/a = 12$ for $\beta = 3.8$. The values of c_{SW} are slightly displaced for better clarity.

the fermion fields is implemented only at 1-loop, resulting in additional $O(ag_0^4)$ effects. We see that the $\beta = 3.3$ result for the coupling in our discretization lies above the value at $a = 0.09\text{fm}$, while the $\beta = 3.4$ is below. This suggests that the β corresponding to $a = 0.09\text{fm}$ in our discretization is in the range $[3.3, 3.4]$.

6 Conclusions

In this paper we have determined c_{SW} for $N_f = 3$ lattice QCD with the tree-level Symanzik-improved gauge action. The result of our determination is the interpolation formula

$$c_{\text{SW}}(g_0^2) = \frac{1 - 0.1921 g_0^2 - 0.1378 g_0^4 + 0.0717 g_0^6}{1 - 0.3881 g_0^2}, \quad (6.1)$$

which may be taken as a definition of the lattice action. While our determination was performed at fixed $L/a = 8$, we performed a finite volume check at $\beta = 3.8$ and found no significant change in c_{SW} .

In addition to a determination of c_{SW} , we have calculated a renormalized L -dependent coupling at $\beta = 3.3$ and 3.4 and compared with an alternative $N_f = 3$ discretization. This determination suggests that the bare coupling corresponding to $a \approx 0.09\text{fm}$ in our discretization is located in the interval $\beta \in [3.3, 3.4]$, indicating that our c_{SW} determination spans the range of desired lattice spacings.

L/a	β	c_1	c_{SW}	c_F	κ	$a(\text{fm})$	$\bar{g}^2(L)$	MDU
8	1.9	-0.331	1.715	0.972168	0.1377	0.090	6.829(26)	45614
8	3.3	-1/12	2.127114	0.970424	0.137017	-	7.381(72)	21904
8	3.4	-1/12	1.986246	0.971294	0.137553	-	6.225(21)	38408

Table 3: $N_f = 3$ results for the Wilson flow coupling $\bar{g}^2(L)$ from Ref. [32] using the Iwasaki gauge action and our discretization. We take the parameters and the scale determination from Ref. [31], while κ was taken from Ref. [20] and found to give $aM \approx 0$. For these simulations only, we set $T = L$ with boundary fields $C_k = C'_k = 0$.

Acknowledgments

It is a pleasure to thank Rainer Sommer and Martin Lüscher for numerous and very helpful discussions and Rainer Sommer for a careful reading of an earlier version of this manuscript. We are also grateful to Hubert Simma and Christian Wittemeier who kindly provided us with their measurement code. The simulations have been done on the thqcd2 installation at CERN. We want to thank the IT department for essential support.

References

- [1] K. Symanzik, *Continuum limit and improved action in lattice theories. 1. Principles and ϕ^4 theory*, *Nucl. Phys.* **B226** (1983) 187.
- [2] K. Symanzik, *Continuum limit and improved action in lattice theories. 2. $O(N)$ nonlinear sigma model in perturbation theory*, *Nucl. Phys.* **B226** (1983) 205.
- [3] M. Lüscher and P. Weisz, *On-shell improved lattice gauge theories*, *Commun. Math. Phys.* **97** (1985) 59.
- [4] K. G. Wilson, *Confinement of quarks*, *Phys. Rev.* **D10** (1974) 2445–2459.
- [5] B. Sheikholeslami and R. Wohlert, *Improved continuum limit lattice action for QCD with Wilson fermions*, *Nucl. Phys.* **B259** (1985) 572.

- [6] M. Lüscher, S. Sint, R. Sommer, P. Weisz, and U. Wolff, *Nonperturbative $O(a)$ improvement of lattice QCD*, *Nucl.Phys.* **B491** (1997) 323–343, [hep-lat/9609035].
- [7] **ALPHA** Collaboration, K. Jansen and R. Sommer, *$O(a)$ improvement of lattice QCD with two flavors of Wilson quarks*, *Nucl. Phys.* **B530** (1998) 185–203, [hep-lat/9803017].
- [8] **ALPHA** Collaboration, M. Della Morte et al., *Scaling test of two-flavor $O(a)$ -improved lattice QCD*, *JHEP* **0807** (2008) 037, [arXiv:0804.3383].
- [9] M. Lüscher and P. Weisz, *On-Shell Improved Lattice Gauge Theories*, *Commun.Math.Phys.* **97** (1985) 59.
- [10] S. Necco, *Universality and scaling behavior of RG gauge actions*, *Nucl. Phys.* **B683** (2004) 137–167, [hep-lat/0309017].
- [11] M. Lüscher, S. Sint, R. Sommer, and P. Weisz, *Chiral symmetry and $O(a)$ improvement in lattice QCD*, *Nucl. Phys.* **B478** (1996) 365–400, [hep-lat/9605038].
- [12] M. Lüscher, R. Narayanan, P. Weisz, and U. Wolff, *The Schrödinger functional: A renormalizable probe for nonabelian gauge theories*, *Nucl. Phys.* **B384** (1992) 168–228, [hep-lat/9207009].
- [13] S. Sint, *On the Schrödinger functional in QCD*, *Nucl. Phys.* **B421** (1994) 135–158, [hep-lat/9312079].
- [14] S. Aoki, R. Frezzotti, and P. Weisz, *Computation of the improvement coefficient $c(SW)$ to one loop with improved gluon actions*, *Nucl.Phys.* **B540** (1999) 501–519, [hep-lat/9808007].
- [15] **JLQCD** Collaboration, N. Yamada et al., *Non-perturbative $O(a)$ -improvement of Wilson quark action in three-flavor QCD with plaquette gauge action*, *Phys. Rev.* **D71** (2005) 054505, [hep-lat/0406028].
- [16] **CP-PACS, JLQCD** Collaboration, S. Aoki et al., *Nonperturbative $O(a)$ improvement of the Wilson quark action with the RG-improved gauge action using the Schrodinger functional method*, *Phys.Rev.* **D73** (2006) 034501, [hep-lat/0508031].
- [17] **ALPHA** Collaboration, F. Tekin, R. Sommer, and U. Wolff, *Symanzik improvement of lattice QCD with four flavors of Wilson quarks*, *Phys.Lett.* **B683** (2010) 75–79, [arXiv:0911.4043].

- [18] N. Cundy et al., *Non-perturbative improvement of stout-smearred three flavour clover fermions*, *Phys.Rev.* **D79** (2009) 094507, [[arXiv:0901.3302](#)].
- [19] M. Lüscher and P. Weisz, *$O(a)$ improvement of the axial current in lattice QCD to one loop order of perturbation theory*, *Nucl. Phys.* **B479** (1996) 429–260, [[hep-lat/9606016](#)].
- [20] M. Lüscher and S. Schaefer, *Lattice QCD with open boundary conditions and twisted-mass reweighting*, *Comput.Phys.Commun.* **184** (2013) 519–528, [[arXiv:1206.2809](#)].
- [21] S. Duane, A. D. Kennedy, B. J. Pendleton, and D. Roweth, *Hybrid Monte Carlo*, *Phys. Lett.* **B195** (1987) 216.
- [22] M. Hasenbusch, *Speeding up the Hybrid-Monte-Carlo algorithm for dynamical fermions*, *Phys. Lett.* **B519** (2001) 177–182, [[hep-lat/0107019](#)].
- [23] M. Hasenbusch and K. Jansen, *Speeding up lattice QCD simulations with clover-improved Wilson fermions*, *Nucl. Phys.* **B659** (2003) 299–320, [[hep-lat/0211042](#)].
- [24] M. Lüscher and F. Palombi, *Fluctuations and reweighting of the quark determinant on large lattices*, *PoS LATTICE2008* (2008) 049, [[arXiv:0810.0946](#)].
- [25] M. Clark and A. Kennedy, *Accelerating dynamical fermion computations using the rational hybrid Monte Carlo (RHMC) algorithm with multiple pseudofermion fields*, *Phys.Rev.Lett.* **98** (2007) 051601, [[hep-lat/0608015](#)].
- [26] **PACS-CS** Collaboration, S. Aoki et al., *Physical Point Simulation in 2+1 Flavor Lattice QCD*, *Phys.Rev.* **D81** (2010) 074503, [[arXiv:0911.2561](#)].
- [27] I. P. Omelyan, I. M. Mryglod, and R. Folk, *Symplectic analytically integrable decomposition algorithms: classification, derivation, and application to molecular dynamics, quantum and celestial mechanics simulations*, *Computer Physics Communications* **151** (2003), no. 3 272 – 314.
- [28] **ALPHA** Collaboration, U. Wolff, *Monte Carlo errors with less errors*, *Comput. Phys. Commun.* **156** (2004) 143–153, [[hep-lat/0306017](#)].
- [29] M. Lüscher, *Properties and uses of the Wilson flow in lattice QCD*, *JHEP* **1008** (2010) 071, [[arXiv:1006.4518](#)].

- [30] **ALPHA** Collaboration, S. Schaefer, R. Sommer, and F. Virotta, *Critical slowing down and error analysis in lattice QCD simulations*, *Nucl.Phys.* **B845** (2011) 93–119, [[arXiv:1009.5228](#)].
- [31] **PACS-CS** Collaboration, S. Aoki et al., *2+1 Flavor Lattice QCD toward the Physical Point*, *Phys.Rev.* **D79** (2009) 034503, [[arXiv:0807.1661](#)].
- [32] P. Fritzsche and A. Ramos, *The gradient flow coupling in the Schrödinger Functional*, [arXiv:1301.4388](#).